International Journal of Chemistry, Mathematics and Physics (IJCMP)
[Vol-10, Issue-2, Apr-Jun, 2026]
https://dx.doi.org/10.22161/ijcmp.10.2.2
ISSN: 2456-866X

Unmanned Aerial Vehicle Automatic Illumination System (Auto-Zoom Illumination Optical System)

Ching Chih-Yen

Guangzhou Institute of Science and Technology, Guangzhou, Guangdong, China
Email: jackaldollars@hotmail.com

Received: 15 Apr 2026; Received in revised form: 13 May 2026; Accepted: 18 May 2026; Available online: 22 May 2026

Abstract**—** *In planetary surface and underwater reconnaissance, UAVs are critical. This study proposes an automatic zoom illumination system for extraterrestrial surface exploration, leveraging the inverse-square relationship between illuminance and distance. The investigation is divided into two parts: the illuminance–distance relationship and the zoom optical system. In part one, the inverse-square law $E=I/r^2$ is experimentally verified using five LED downlights of different powers. At distances of 1 m and 2 m, the measured illuminance values closely match the theoretical predictions, with an average error of only 2.3%. This confirms that illuminance decreases with the square of distance. Thus, when a UAV at a fixed altitude encounters terrain depressions, the power adjustment needed to maintain illuminance can be calculated from the laser-measured distance.The second part addresses the zoom optical system. To increase local illuminance, one can raise the LED power to boost luminous flux, using $E=\Phi/A$. With a maximum efficacy of 150 lm/W, the required power can be derived. If the needed power exceeds the LED's rating, one may use a spherical lens to concentrate light or a laser system. This work focuses on the lens approach. Varying the LED–lens distance changes the refraction angle, adjusting beam divergence and concentrating light. Optical simulations optimize floodlight uniformity and spotlight efficiency, enabling a zoom beam from focused to wide. The relationships among source–lens separation, distance, and illuminance are determined.*

Keywords**— *Automatic zoom illumination, Inverse square law of illuminance, LED light source, Unmanned aerial vehicle (UAV), Zoom optical system.***

I. INTRODUCTION

Current approaches for applying LEDs to illumination generally include: (i) arranging packaged LEDs directly in an array so that the light diverges freely; (ii) placing an LED inside a reflector and shaping the reflector to direct the reflected light toward a target; (iii) using the principles of total internal reflection and refraction of a lens to guide the light forward. Through various combinations of these design methods, light can be effectively concentrated or directed to a specific location for a particular purpose. However, since these optical elements do not change their shape, the beam is fixed, resulting in the drawback that only one beam requirement can be met. Depending on the application, the required illumination area may differ: sometimes a focused spotlight beam is needed to send light to a great distance, as with lighthouses and stage lights; at other times a divergent floodlight is needed to illuminate a large area, as with indoor lighting and searchlights. A lighting system with a zoom function can adjust the illumination range according to demand, enabling the same device to produce either a concentrated beam or wide-area illumination. Therefore, a zoomable illumination design saves space and cost, and is truly valuable for application as well as worthy of research. In this technologically advanced era, UAV equipment and machines have progressed enormously. Reconnaissance missions on planetary surfaces must rely on unmanned machines. Previously, space illumination merely lit up a certain region or a portion of an area for observation, which often resulted in excessively high illuminance and glare, thereby affecting detection and observation. For example, when a UAV cruises at a specific altitude (fixed flight height) and inspects the ground surface, encountering uneven terrain

may prevent a camera from capturing clear images of depressed areas without changing the flight height. In such a situation, an automatic optical zoom illumination system can solve the problem of insufficient illuminance due to excessive distance.

This study combines a laser rangefinder with an automatic optical zoom illumination system. With the UAV flying at a safe altitude, the laser rangefinder returns distance data, after which a control chip evaluates and determines the adjustment of the distance between the light source and the lens in the optical system, altering the refraction angle of the light and converging the rays to increase the illuminance in that region. The Elite 1600 ARC laser rangefinder telescope has a maximum range of 1450 m and a light weight of only 343 g, making it easy for a UAV to carry.

Assuming the UAV cruises at an altitude of 10 m, with the illuminance standard for indoor reading of 600 lx, an LED luminous efficacy of 150 lm/W, and a beam angle of 120° (without passing through any lens), the required luminous flux would be 188,496 lm, corresponding to an LED power of about 1256 W to meet the illuminance value over that area.

An LED light source of 1256 W is extremely powerful. In practical terms, the heat dissipation for such an LED must be very efficient, and the heat-dissipation structure would certainly be quite bulky. A reconnaissance UAV has limited payload capacity, so the weight of the heat-dissipation mechanism must be reduced. At present, the only solution lies in the optical system. This paper temporarily disregards the heat-dissipation issue. Since all optical elements used are much larger than the wavelength, and the influence of edge diffraction is minimal, the analysis is conducted based on the theory of geometrical optics.

II. RELATIONSHIP BETWEEN ILLUMINANCE, DISTANCE, AND BEAM ANGLE

In photometry, illuminance (E) is defined as the luminous flux density incident on a surface per unit area, with units of lumen per square meter (lux). Its formula is equation 1(F: luminous flux; m: meter; I: luminous intensity; r: distance from the point source to the surface [unit: m]). Luminous intensity (I), considering a point source, is the luminous flux density per unit solid angle in a given direction, with units of lumen per steradian (cd). Its formula is equation 2. The unit solid angle Ω is calculated as equation 3, where θ is defined as shown in Fig. 1. With these relationships, we can determine the variations of luminous flux, illuminance, luminous intensity, and beam angle at different distances [1,2].

$$E = F / m^2 = I / r^2 \quad (1)$$

$$I = F / \Omega \quad (2)$$

$$\Omega = 2\pi (1 - \cos\theta) \quad (3)$$

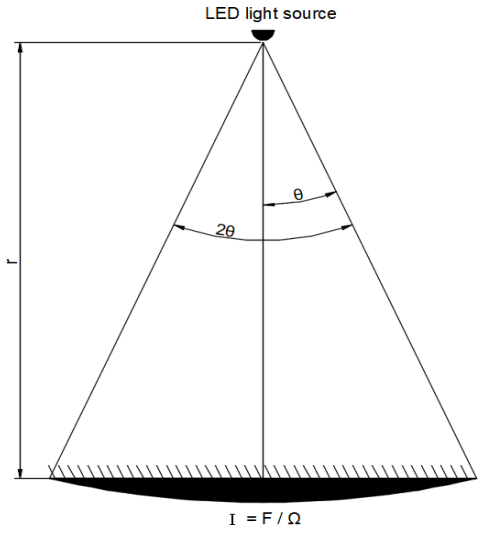

Fig. 1 Schematic diagram of the emission angle and height of the LED light source

2.1 Illuminance variation under different experimental conditions (Inverse square law of illuminance – verification)

Among the wide variety of luminaires on the market, we selected the five most readily available LED downlights for testing: a 7.5 cm 3.3 W downlight, a 7.5 cm 7.7 W downlight, a 9.5 cm 7 W downlight, a 9.5 cm 8.3 W downlight, and a 9.5 cm

11.3 W downlight. After passing through a TIR lens, the beam angle was 25°. The illuminance meter was fixed to an extendable rod, and the distances were set to 1 m and 2 m. The illuminance values were measured at a distance of 1 m and at a distance of 2 m.

Experimental results: for the 7.5 cm 3.3 W downlight, the illuminance at 1 m was approximately 570 lx, and at 2 m it was approximately 146 lx; for the 7.5 cm 7.7 W downlight, the illuminance at 1 m was approximately 2.2 klx, and at 2 m it was approximately 563 lx; for the 9.5 cm 7 W downlight, the illuminance at 1 m was approximately 1.94 klx, and at 2 m it was approximately 497 lx; for the 9.5 cm 8.3 W downlight, the illuminance at 1 m was approximately 2.73 klx, and at 2 m it was approximately 701 lx; for the 9.5 cm 11.3 W downlight, the illuminance at 1 m was approximately 3.58 klx, and at 2 m it was approximately 914 lx. Table 1 lists the illuminance values of the five LED downlights at different distances.

Table 1 Illuminance values of five LED downlights at different distances

Type\istance	Distance 1m(lx)	Distance 2m(lx)
A. 7.5cm 3.3W	570	146
B. 7.5cm 7.7W	2200	563
C. 9.5cm 7W	1940	497
D. 9.5cm 8.3W	2730	701
E. 9.5cm 11.3W	3580	914

2.2 Application of the inverse square law of illuminance (determination of error)

When applying the inverse square law of illuminance, the error ratio between the calculated and measured illuminance values was 2.4% for A, 2.3% for B, 2.4% for C, 2.6% for D, and 2.1% for E, with an overall average error ratio of 2.4% (Table 2). This indicates that the deviation between the actually measured illuminance values and those derived from the inverse square law formula is small, and the formula can be used to estimate illuminance values at different distances.

Table 2 Calculated illuminance values at a distance of 2 m and error ratios

Type \istance	Distance 1m(lx)	Distance 2 m (lx) (calculated)	Error %
A. 7.5cm 3.3W	570	142.5	2.4
B. 7.5cm 7.7W	2200	550	2.3
C. 9.5cm 7W	1940	485	2.4
D. 9.5cm 8.3W	2730	682.5	2.6
E. 9.5cm 11.3W	3580	895	2.1

III. LIGHT SOURCE EMISSION ANGLE CONTROL OPTICAL SYSTEM

3.1 Design concept

By appropriately adjusting a light source in combination with a hyperboloid reflector, uniform large-area illumination can be formed in the forward direction. If the light source moves forward along the axis, the angle of incidence on the reflective surface decreases, and the angle of reflection decreases accordingly, so that the angle between the emitted rays and the horizontal becomes increasingly smaller. As shown in Fig. 2, an LED light source is placed inside a hyperboloid reflector, and the emitted light is divided into two parts: the first part originates from the light reflected by the reflector (denoted as a), and the second part is the directly emitted light (denoted as b). Ray b strikes point P on the reflective surface. Ray c is defined as the ray that just grazes the outermost edge of the reflector, making an angle θ_1 with the horizontal. Rays with an angle greater than θ_1 will not be emitted directly; therefore, ray c can determine the maximum illumination range.

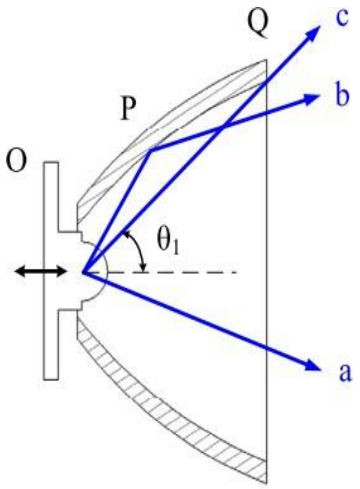

Fig. 2 Schematic diagram of ray tracing for rays a, b, c before the light source moves.

If the light source is moved forward along the optical axis, as shown in Fig. 3, ray b that strikes point P on the reflective surface undergoes a smaller angle of incidence and, consequently, a smaller angle of reflection. Due to the hyperboloid shape, the light will be emitted at an angle progressively closer to the horizontal, gradually forming a concentrated illumination in the forward direction and achieving a zoom effect.

However, compared with other curved surfaces, the hyperboloid has a larger opening. As the light source moves forward, many rays diverge directly and are not controlled by the reflective surface. In Fig. 2, before the light source moves, ray c makes an angle θ_1 with the horizontal; after the movement, the angle becomes θ_2 as shown in Fig. 3. Since θ_2 is larger than θ_1, the angular range of the directly emitted rays increases. Such diverging rays can enlarge the illumination area, but moving the light source relative to the reflective surface actually provides a focusing function [3].

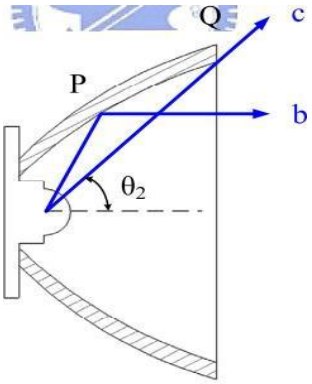

Fig. 3 Schematic diagram of ray tracing for rays a, b, c after the light source moves.

It can be seen that when the light source moves along the optical axis, the range of directly emitted light can be controlled. A spherical lens is added in front of the reflector, as shown in Fig. 4. The function of this spherical lens arises from mechanical considerations: when an excessive amount of light is directly emitted without passing through the lens, ray c, which grazes the reflector, would originally be emitted directly; after the lens is introduced, it is refracted and emitted forward. The reflector can intercept and reflect the light, converging it toward the lens. When the reflector is unable to reflect the light emitted by the source into parallel rays, the spherical lens must be relied upon to compensate. With both a reflector and a spherical lens, one must consider issues such as the reflective system, refractive system, vergence, refractive power, and focal length. The light refracted by the lens emerges as plane waves. Using the principle of reversibility of light, the focal length of the spherical lens can be calculated (spherical aberration is temporarily ignored; in illumination optical systems, the effect of spherical aberration is relatively minor and can be neglected for the time being). Since the emission angle of an LED

light source is fixed—currently most LED light sources have an emission angle of 120 degrees—if the light source is moved backward along the optical axis, a crossed divergence phenomenon will occur due to the limitation imposed by the LED's emission angle, as shown in Fig. 5. Therefore, the light source must be moved along the optical axis toward the center of curvature. During this movement, the light directly emitted through the lens increases the emission angle and range, as illustrated in Fig. 6. Before the movement, the angle between ray c and the optical axis is θ_5, and after the movement it is θ_5'; θ_5' is larger than θ_5. Similarly, θ_6' is larger than θ_6. In other words, with the lens and reflector fixed, the emission angle is adjusted by moving the LED light source along the optical axis toward the center of curvature, thereby forming a zoom optical system.

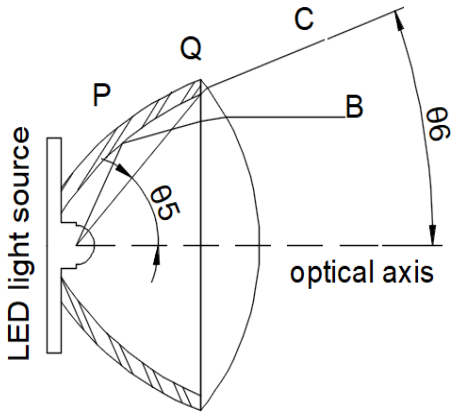

Fig. 4 A spherical lens installed in front of the reflector

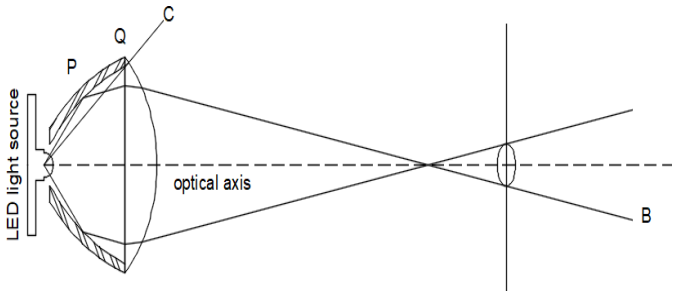

Fig. 5 The light source moves backward along the optical axis, resulting in a crossed divergence phenomenon.

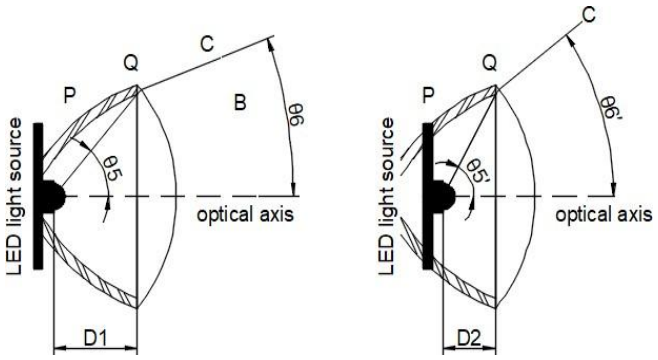

Fig. 6 Before movement (left) and after moving rightward along the optical axis (right).

3.2 Focal point and focal length of a spherical lens

Optical systems are often described by several special points, among which the most important is the focal point. The characteristics of the focal point are closely related to optical infinity; in other words, they pertain to rays that are incident on or emerge from the system parallel to the optical axis (with a vergence of 0) [4]. The vergence equation is explained in Section 3.2.1.

Incident light emitted from a point on the axis, after refraction at a spherical interface, emerges as a plane wave. The focal length is the object distance when the image is at optical infinity. Using the vergence equation V=0, we obtain U=−P. Since U=n1/u, and the object distance u at this point is the focal length f, we have equation 4. The focal point of a converging surface is real, as shown in Fig.7.

$$f = -\frac{n1}{P} \quad (4)$$

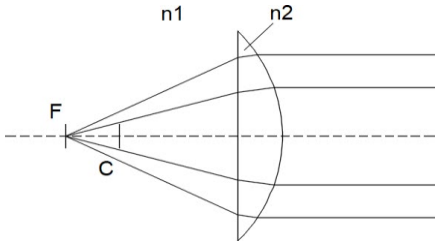

Fig. 7 By the principle of reversibility of light, the focal point F of a converging interface is real.

3.2.1 Vergence U & V and refractive power P

3.2.1.1Vergence

We know that in a homogeneous medium, a diverging spherical wavefront originating from a point object becomes less divergent as it travels away from the object. Conversely, a converging spherical wavefront leaving an optical system becomes more convergent as it approaches the point image. After the converging wavefront passes through the point image, it once again becomes a diverging spherical wavefront.

We use the concept of vergence to describe the degree of convergence or divergence of a spherical wavefront at different distances. A spherical surface with large curvature has a large degree of vergence, while one with small curvature has a small degree of vergence. Furthermore, vergence must carry a sign to distinguish whether the wavefront is converging or diverging. A positive value represents converging vergence, and a negative value represents diverging vergence. If the direction of measurement is the same as the direction of light propagation, the radius of curvature takes a positive value; conversely, if the direction of measurement is opposite to that of light propagation, the radius of curvature takes a negative value, as shown in Fig. 8. The formula is equation 5, where V represents the vergence of the spherical wavefront, r denotes the radius of curvature of the spherical surface (in meters), and n is the refractive index of the medium.

$$V = \frac{n}{r} \quad (5)$$

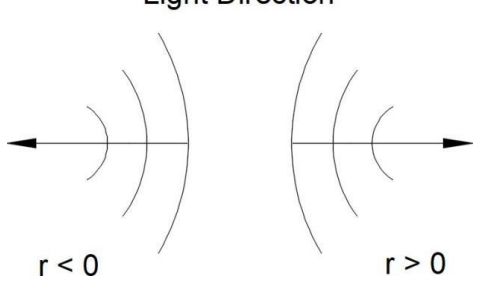

Fig. 8 Sign convention for the radius of curvature.

3.2.1.2 Diopter

Diopter (or dioptric power) is the unit for measuring the refractive power of a lens or curved mirror. The focal length *f* indicates the magnitude of the refractive power: the shorter the focal length, the greater the refractive power. Myopia is caused by an excessively strong refractive power of the eye, while hyperopia results from an overly weak refractive power.

When incident light is incident on a spherical lens surface along the optical axis, because the optical axis is simultaneously the normal to both surfaces, the angles of incidence and refraction are both 0° for the two spherical surfaces. Therefore, light incident along the optical axis will not be deviated after passing through the lens, and the rays leaving the lens still propagate along the optical axis. In a thin-lens optical system, the optical properties depend on the refractive powers

of the front and rear surfaces, as well as the refractive index and thickness of the lens. If the central thickness of the lens is sufficiently small that the change in vergence of the light ray when traveling from the first surface to the point of incidence on the second surface is very small, the lens can be regarded as a thin lens. The refractive power of a thin lens is the sum of the spherical surface powers of the two surfaces, as given in equation 6.*P* represents the refractive power of the thin lens, while P_1 and P_2 are the spherical surface powers of the first and second surfaces, respectively. The converging or diverging property of a thin lens in air is independent of the lens shape and the direction of light propagation through the lens.

$$P = P_1 + P_2 \qquad (6)$$

The relationship between spherical surface power, refractive index, and radius of curvature is expressed as the difference between the two refractive indices n_2 and n_1, divided by the radius of curvature r, as shown in equation 7, where r_1 and r_2 are the radii of curvature of the first and second surfaces, n is the refractive index of the lens, and the media before and after the lens are both air. The corresponding formula is equation 8. This formula is also the so-called lensmaker's equation, which is the reciprocal of the focal length f:

$$P = \frac{n_2 - n_1}{dx} \qquad (7)$$

$$P = \frac{n-1}{r_1} + \frac{1-n}{r_2} = \frac{1}{f} = (n-1)\left(\frac{1}{r_1} - \frac{1}{r_2}\right) \qquad (8)$$

3.3 Relationship between the light source–lens distance and the emission angle

After determining the focal length and focal point of the lens using the vergence equation, according to the design concept described earlier, the light source must be moved along the optical axis toward the center of curvature to change the emission angle. As shown in Fig. 9, the light source is initially placed at the focal point F1 of the lens, so that the exiting rays leave the lens as plane waves. Because the ray tracing through a spherical lens is symmetric—in other words, the ray tracing above the optical axis is identical to that below the optical axis—for ease of explanation, we take the ray tracing above the optical axis as an example. Rays a1, a2, and a3 originate from the focal point and strike the lens. Due to the influence of the refractive index, they are deviated and then leave the lens as plane waves. The angle between ray a1 and the horizontal is θ6−a. When the light source moves along the optical axis toward the center of curvature to position Q1, as shown in Fig. 10, rays a1, a2, and a_3 are deviated in the direction opposite to the optical axis. At this time, the angle between ray a1 and the horizontal (optical axis) is θ6−b. Since θ6−b is larger θ6−a, the rays a1, a2, and a3, which were initially parallel to the optical axis, are now deviated outward, and the angular spread of the rays emerging from the lens naturally increases.

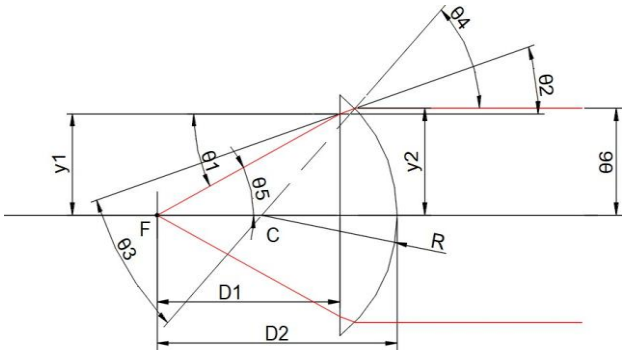

Fig. 9 Focal point of the optical system and positions of various incidence and refraction angles.

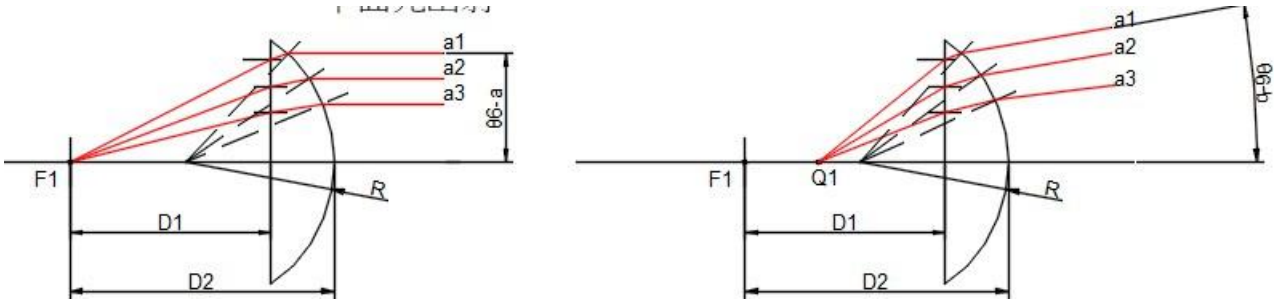

Fig. 10 Ray tracing when the light source is at the focal point (left) and after moving along the optical axis to Q_1 (right).

As shown in Fig. 9, when light undergoes refraction, it follows the law of refraction. An incident ray striking the lens (the first refracting interface) makes an angle of incidence θ_1, and upon deviation produces θ_2, which is the angle of refraction. The refracted ray then strikes the lens (the second refracting interface), making an angle of incidence θ_3, and upon deviation produces the angle of refraction θ_4. The angle between the incident ray FA_1 and the optical axis is θ_5, where $A_1$is a fixed point of incidence. From Fig. 9 it can be seen that the normal at A_1 is parallel to the optical axis, and θ_1 and $\theta_5$are alternate interior angles. $\theta_6$is the angle between the emergent ray and the horizontal optical axis. When the starting position of the incident ray is moved sequentially from the focal point F toward the center of curvature C, it is observed that the angular variations of $\theta_1$and $\theta_5$increase and decrease synchronously.

3.3.1 Ray tracing through multiple surfaces

When calculating the propagation of light through multiple surfaces consecutively, it is more convenient to use another form of the paraxial formula. As shown in Fig. 11, a paraxial ray is incident on a surface, and the height of the point of incidence from the optical axis is y. The distances along the optical axis from the ray intersection points before and after refraction are l and l'. Because the paraxial region is a very small region near the optical axis, the height y in this context is an assumed extension of the paraxial region. However, since all heights and angles are eliminated from the paraxial expressions, using finite values for the heights and angles for the focal distances does not affect the accuracy of the expressions. For optical systems of moderate aperture, these fictitious heights and angles can yield reasonably approximate values when applied in trigonometric calculations. In the paraxial region, every surface is nearly planar, and all angles approximate their sines and tangents. Therefore, the inclination angles shown in Fig. 11 can be expressed as $u=-y/l$ and $u'=-y/l'$, or $l=-y/u$ and $l'=-y/u'$ [5].

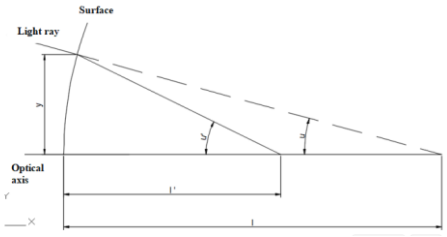

Fig. 11 Relationship of paraxial rays

If these values of i and i' are substituted into equation (9), we obtain equation (10). Multiplying both sides by y yields the formula for the slope angle after refraction, equation (11). It is convenient to introduce the surface curvature $C=1/R$ as a replacement, as shown in equation (12) [6]. To continue the calculation for the next surface, a set of transfer equations is required. As shown in Fig. 12, an optical system consisting of two surfaces separated by a distance t. The slope angle of the ray after refraction by surface 1 is $u1'$, and the ray heights at the surfaces are $y1$and $y2$, respectively. Under paraxial calculation, the difference in heights is $tu1'$; therefore, we obtain equation (13) [7,8]. The slope angle of the ray incident on the second surface is the same as that of the ray refracted by the first surface, which leads to the second transfer equation $u2=u1'$or $u2=n1'u1'$. These equations can be used to determine the image position and size of an optical system. The paraxial ray heights and angles can be scaled proportionally, with the scaled result representing the data of another ray [9,10,11].

$$\frac{n'}{l'} = \frac{(n'-n)}{R} + \frac{n}{l} \quad (9)$$

$$\frac{n'u'}{y} = \frac{-(n'-n)}{R} + \frac{nu}{y} \quad (10)$$

$$n'u' = nu - y\frac{(n'-n)}{R} \quad (11)$$

$$n'u' = nu - y(n'-n)C \quad (12)$$

$$y_2 = y_1 + tu'_1 = y_1 + t\frac{n'_1 u'_1}{n'_1} \quad (13)$$

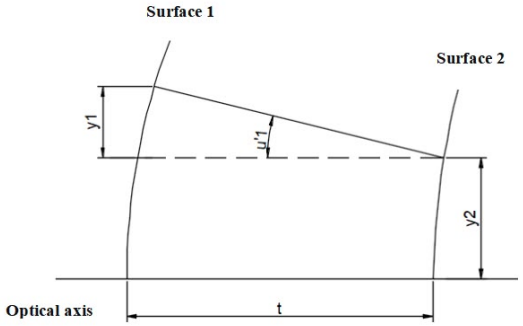

Fig. 12 Paraxial ray undergoing surface transfer.

3.3.2 Verification by applying the above formulas

As shown in Fig.13, suppose there is a lens (refractive index n=1.55), a plano-convex lens with a radius of curvature of 30 mm and a diameter of 49 mm. Using equation 2.5, the focal length F of the lens is found to be 53.15 mm. Preset the incident point at a height of 20.62 mm above the optical axis, and calculate the angle of incidence θ_1, the angle of refraction θ_2, the distance from the point of incidence on the second surface to the optical axis y_2, the angle of incidence inside the lens θ_3, the angle of refraction at the second surface θ_4, the angle between the emergent ray and the horizontal optical axis θ_6, and the angle between the light source and the optical axis θ_5, as shown in Fig. 9. We substitute the parameters as listed in Table 3, and sequentially decrease the focal length in steps of 10 mm to observe the variations of each angle.

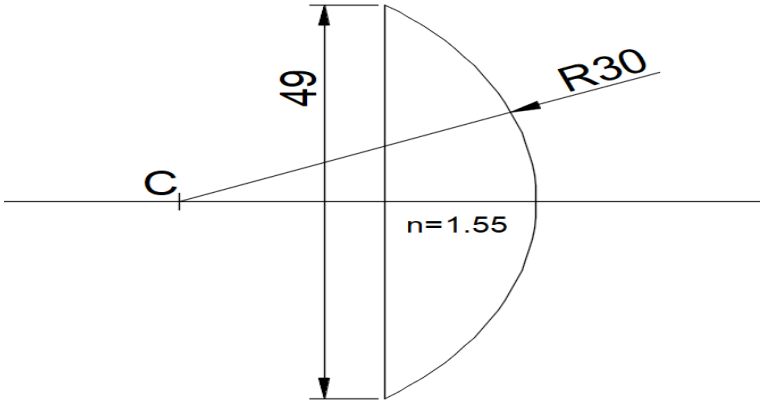

Fig. 13 Schematic diagram of the plano-convex lens specifications (radius of curvature 30 mm, diameter 49 mm).

Table 3 Data obtained from ray tracing after varying the focal length, using the lens example of Fig. 13.

Angle Ag\Focal length D1	40.46mm	30.46mm	20.46mm	10.46mm
θ1	27 °	34.09 °	45.21 °	63.09 °
θ2	18 °	21.1 °	27.12 °	35.02 °
θ3	28.38 °	25.68 °	20.4 °	13.39 °
θ4	46.38	42.55 °	31.53 °	20.78 °
θ5	27 °	34.09 °	45.21 °	63.09 °
θ6	0 °	4.23 °	15.99 °	27.63 °
y1	20.62mm	20.62mm	20.62mm	20.62mm
y2	21.72mm	21.86mm	22.13mm	22.44mm
D1	40.46mm	30.46mm	20.46mm	10.46mm
D2	53.15mm	53.15mm	53.15mm	53.15mm

When the light source moves away from the focal point F and travels along the optical axis toward the center of curvature C, as shown in Fig. 14a, at a focal length of 34.46 mm the angle θ_6 begins to bend slightly upward by 1.55°, and θ_4, which was originally parallel to the optical axis, also gradually bends upward. From Table 3, when the emergent ray was initially horizontal to the optical axis, θ_4 was 46.38°, and when the focal length becomes 30.46 mm the upward bending angle reduces to 45.01°. The farther the light source is from the focal point, the larger the bending angle. Fig. 14b shows the distinct change in θ_6 more clearly, increasing from 1.55° to 2.52°. In other words, the shorter the focal length, the more pronounced the deviation. When the focal length is 30.46 mm, the angle between the emergent ray and the optical axis deviates upward from the horizontal by 4.23°; when the focal length is 20.46 mm, it deviates upward by 16°; when the focal length is 10.46 mm, it deviates upward by 28°. As the focal length was shifted by 30 mm, the emergent ray angle actually deviated by 28°, meaning that for every 1 mm decrease in focal length, the angle between the emergent ray and the optical axis increases by approximately 1°. Through the above formula calculations and verification, we can accurately determine the relationship between the change in distance between the focal point and the lens and the angle between the emergent ray and the optical axis.

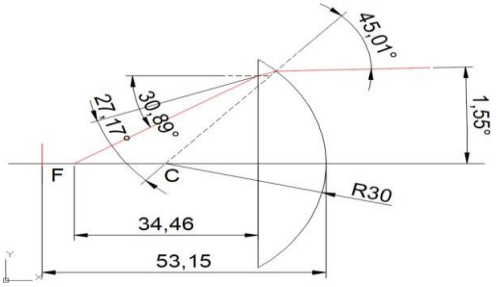

Fig. 14a Angular data when the focal length is 34.46 mm

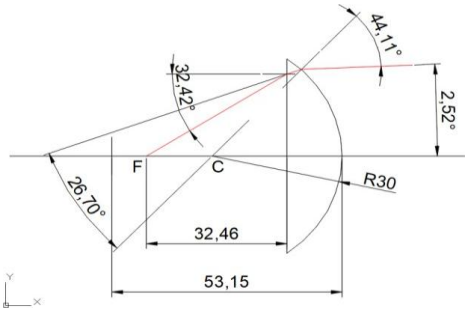

Fig. 14b Angular data when the focal length is 32.46 mm

IV. ASSUMPTION

Based on the preceding description and verification, we understand the relationship between the LED light source and the lens in the automatic zoom optical system, as well as the method for calculating the overall optical system in relation to the environment, distance, and emission angle. If this entire system is applied to detection technology, as shown in Fig. 15, it is assumed that the optical system is installed on a reconnaissance UAV. For ease of calculation, the initial cruising altitude is preset to 5m, the target illuminance on the illuminated surface is preset to 500 lx, and a 100 W LED light source with a luminous efficacy of 140 lm/W is used, yielding a luminous flux of 14,000 lm. At the original cruising altitude of 5 m, the beam angle is 70°.

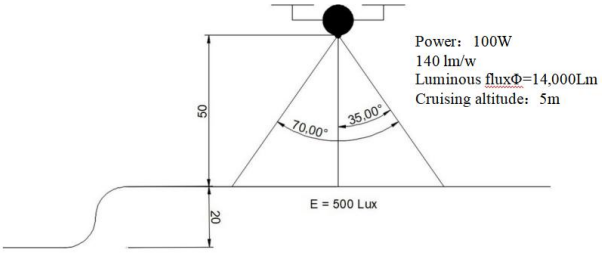

Fig. 15 Relationship between the emission angle and illuminance of the UAV at an altitude of 5 m.

When a depressed area is encountered ahead, with the depressed area located 7 m from the UAV, and the laser rangefinder receives a return signal that differs from the original altitude, a recalculation is performed to determine whether to adjust the output power or change the distance between the LED light source and the lens, so as to maintain the illuminance E on the illuminated surface at 500 lx. Based on the distance of 7 m measured by the rangefinder, the luminous intensity I is calculated using equation (1) (equation 14). Substituting the distance and illuminance yields I=24,500 cd. Then, substituting the luminous flux into equation (3) gives cosθ, as in equation 15, and the beam angle is 2cosθ=50∘, as shown in Fig. 16.

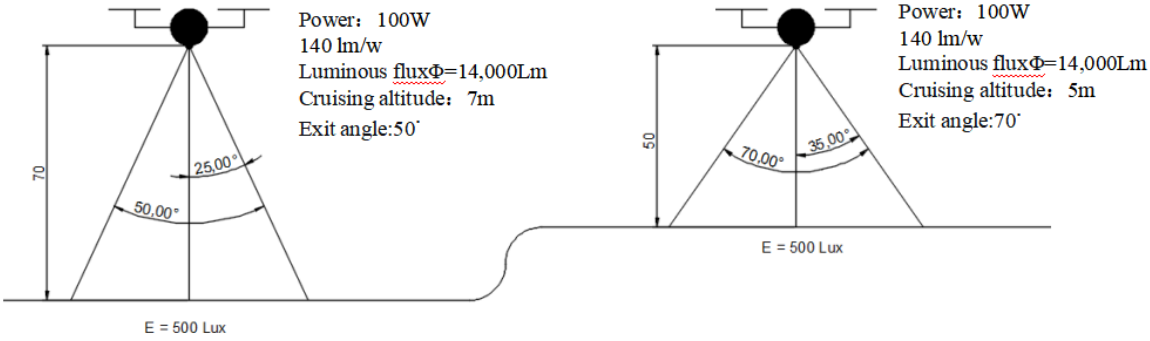

Fig. 16 Data at a UAV cruising altitude of 7 m (left) and data at a cruising altitude of 5 m (right).

Next, we turn to the optical system. The lens used in this optical system is a plano-convex lens with a radius of curvature R_1 of 30 mm, made of glass with a refractive index n=1.55, as shown in Fig. 17. The distance t between the first surface R_1 and the second surface R_2 is 12.69 mm. Using Eqs. (9)–(13), the incidence position on the first surface is found to be y_1=20.62 mm, and the height of the ray after refraction at the second surface is y_2=22.38 mm. After refraction, the angle between the ray and the optical axis is θ_6=25.04°, and the sum of the angles above and below the optical axis is 50°. Through the above calculation and derivation, when the UAV is at a height of 7 m from the depressed area, it is not necessary to increase the LED light source power; only the focal distance between the LED light source and the lens needs to be adjusted so that the illuminance on the illuminated surface reaches the required 500 lx.

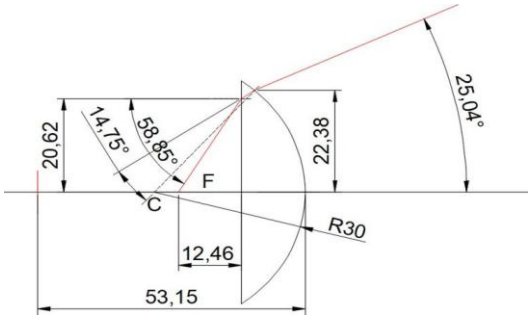

Fig. 17 Internal focal length and various angular data of the optical system when the exit beam angle is 50°.

V. CONCLUSION

This study proposes an automatic zoom illumination system. When environmental conditions change—for example, changes in UAV flight altitude, the depth of a depression, or the illumination distance—one only needs to substitute the changed height into the above formulas to determine the exit angle of the optical system. With this angle, it can be substituted into the formula relating the LED light source and the lens focal length, thereby obtaining the focal length corresponding to that angle. By controlling the focal distance between the LED light source and the lens, the angle between the exit ray and the optical axis is controlled. However, before starting the calculation, one must first consider how to meet the requirement of 500 lx on the illuminated surface: either by increasing the power to raise the total luminous flux, or by changing the focal distance between the LED light source and the lens. In the author's opinion, it is necessary to consider the flight endurance of the UAV. If the output power is increased to raise the total luminous flux in order to meet the illuminance requirement, too much energy will be consumed, leading to insufficient UAV endurance. Moreover, although the illuminance on the illuminated surface meets the required standard, if the illumination area is too small—a minimum spot diameter of 1 m is required—the purpose of clear observation will also be lost. For example, when the altitude is 5 m, based on the above formula calculations, if an illumination area with a diameter of about 1 m is required, the exit angle of the optical system needs to be 12°. When encountering a depressed area at a distance of 7 m from the optical system, the exit angle must be at least 9° to meet the 1 m illumination spot standard. Therefore, before deciding on a course of action, one must first evaluate whether the distance can be preferentially resolved by the optical zoom system. If even a small angle cannot make the illuminance reach the required standard, then the output power should be increased to overcome the problem of insufficient illuminance.

VI. FUTURE PROSPECTS

Regarding future prospects, the automatic zoom illumination optical system in this study is mainly intended for space exploration. It will be of great help and application in space exploration or deep-sea exploration. In the unknown world, humans are full of curiosity about unknown and uncontrollable regions. This study applies the concept of automatic zoom illumination to UAVs, allowing the UAV to capture the terrain more clearly when performing reconnaissance missions, and enabling humans to clearly see the complete terrain during observation. By using a simple flashlight principle, high-quality zoom illumination can be achieved, with a fairly large adjustment range and a small size, offering considerable room for development. If this technology is applied commercially, for controlling the flood angle, stage focusing, and automotive applications, I believe it is a technology with great potential.

REFERENCES

[1] Michael Bass. (Ed.) *Handbook of Optics Volume II-Devices, Measurements and Properties*, 2nd Ed. McGraw-Hill, 1995.
[2] Optronic Laboratories, Inc.
[3] Y.-P. Tsai, *Optical element design for zoom LED illumination systems*, Master's thesis, Institute of Mechanical Engineering, National Chiao Tung University, Hsinchu, 2007 (unpublished).
[4] J.Wang,*Geometrical Optics*,New Wun Ching Developmental Publishing Co., New Taipei City, 2014.
[5] W. J. Smith, *Modern Optical Engineering*, 4th ed., translated by H.-B. Zhou and Y.-F. Cheng .Beijing Chemical Industry Press, Beijing, 2011.
[6] Bass, M., *Handbook of Optics*, Vol. 1, New York, McGrraw-Hill, 1995.

[7] Fischer, RR. E., and B. Tadic-Galeb. *Optical System Design*, New York, McGrraw-Hill, 2000.
[8] Greivenkamp, J., *Field Guide to Geometrical Optics*, Bellingham, WA, SPIE, 2004.
[9] Kingslake, R., *Optical System Design*, Orlando, Academic, 1983.
[10] Smith, W. J., *Modern Lens Design*, New YOrk, McGraw-Hill, 2002.
[11] Smith, W. J., *Practical Optical System Layout*, New York, McGraw-Hill, 1997.